

Role of tree size in moist tropical forest carbon cycling and water deficit responses

Victoria Meakem¹, Alan J. Tepley¹, Erika B. Gonzalez-Akre¹, Valentine Herrmann¹, Helene C. Muller-Landau², S. Joseph Wright², Stephen P. Hubbell^{2,3}, Richard Condit² and Kristina J. Anderson-Teixeira^{1,2}

¹Conservation Ecology Center, Smithsonian Conservation Biology Institute, Front Royal, VA 22630, USA; ²Center for Tropical Forest Science, Smithsonian Tropical Research Institute, Balboa Ancon, Panama, Republic of Panama; ³Department of Ecology and Evolutionary Biology, University of California, Los Angeles, Los Angeles, CA 90095, USA

Summary

Author for correspondence:
Kristina J. Anderson-Teixeira
Tel: +1 540 635 6546
Email: teixeirak@si.edu

Received: 3 March 2017
Accepted: 27 April 2017

New Phytologist (2018) **219**: 947–958
doi: 10.1111/nph.14633

Key words: biomass, drought adaptation, El Niño, tree mortality, tree size, tropical moist forest, woody productivity.

- Drought disproportionately affects larger trees in tropical forests, but implications for forest composition and carbon (C) cycling in relation to dry season intensity remain poorly understood.
- In order to characterize how C cycling is shaped by tree size and drought adaptations and how these patterns relate to spatial and temporal variation in water deficit, we analyze data from three forest dynamics plots spanning a moisture gradient in Panama that have experienced El Niño droughts.
- At all sites, aboveground C cycle contributions peaked below 50-cm stem diameter, with stems ≥ 50 cm accounting for on average 59% of live aboveground biomass, 45% of woody productivity and 49% of woody mortality. The dominance of drought-avoidance strategies increased interactively with stem diameter and dry season intensity. Although size-related C cycle contributions did not vary systematically across the moisture gradient under nondrought conditions, woody mortality of larger trees was disproportionately elevated under El Niño drought stress.
- Thus, large (> 50 cm) stems, which strongly mediate but do not necessarily dominate C cycling, have drought adaptations that compensate for their more challenging hydraulic environment, particularly in drier climates. However, these adaptations do not fully buffer the effects of severe drought, and increased large tree mortality dominates ecosystem-level drought responses.

Introduction

Tropical forests play critical roles in the global carbon and climate cycles. They contain an estimated 34% of terrestrial carbon (C; US DOE, 2012), account for 34% of global gross primary productivity (Beer *et al.*, 2010), and influence climate on local to global scales through their high rates of evapotranspiration (Snyder *et al.*, 2004; Lawrence & Vandecar, 2015). Across the tropics, anticipated changes in the spatial and temporal availability of water (IPCC, 2013) are expected to alter the ecophysiology and composition of forests, with consequent feedbacks to the climate system. Given the importance of tropical forests to the climate system, these feedbacks may be quite significant, yet our understanding of tropical forest responses to water deficit remains limited (e.g. Sitch *et al.*, 2008; Huntingford *et al.*, 2013; Powell *et al.*, 2013; Anderegg *et al.*, 2015; Corlett, 2016). To precisely describe or predict forest responses to climate variation or change, it is necessary to characterize both the exact relationship between tree size and C cycling, and the differential responses of trees of different sizes to hydraulic stress.

Despite a common conception that larger trees dominate tropical forest C cycling (e.g. Fauset *et al.*, 2015; Bastin *et al.*, 2015), there is a surprising paucity of studies quantifying in detail how contributions to key components of forest C budgets – specifically, live aboveground biomass ($C_{ag, live}$), woody productivity ($ANPP_{stem}$) and woody mortality (M) – vary as a function of tree size. The proportional contribution of large trees to total biomass is variable, with contributions of trees ≥ 70 cm diameter at breast height (DBH) ranging up to 45% in neotropical forests (Schiatti *et al.*, 2016, and reference therein). With regards to biomass turnover (i.e. $ANPP_{stem}$ and M), some theoretical work suggests energy or C-flux equivalence across size classes (Enquist *et al.*, 2009), but these predictions do not account for differences in light availability to the different size classes (Muller-Landau *et al.*, 2006a) or deviations from power-law scaling of size–abundance relationships (Coomes *et al.*, 2003; Muller-Landau *et al.*, 2006b). The exact form of the relationship between tree size and ecosystem-level C contributions in tropical forests has yet to be described, and we do not know how this relationship is shaped by climate.

Trees of different sizes respond differently to variation in hydraulic conditions; in tropical forests worldwide, drought tends to have a greater impact on the growth and mortality of large than small trees (Phillips *et al.*, 2010; Bennett *et al.*, 2015). These differences can be quite pronounced; in some cases, drought has actually increased the growth rate of small trees while decreasing the growth rate of large trees (Bennett *et al.*, 2015). The greater drought sensitivity of large tropical trees is likely driven by a combination of the greater hydraulic challenge of lifting water to greater height against the effects of gravity and path length-associated resistance (Ryan *et al.*, 2006; Zhang *et al.*, 2009; McDowell *et al.*, 2011; McDowell & Allen, 2015) and greater abiotic stress associated with an exposed canopy position (Roberts *et al.*, 1990; Nepstad *et al.*, 2007; Bennett *et al.*, 2015). It remains unclear, however, how the more challenging hydraulic situation of larger trees affects forest composition and carbon cycling under nondrought conditions.

Trees exhibit a variety of adaptations to minimize moisture loss during periods of dry season or droughts. Deciduousness is a drought avoidance strategy, whereby leaf loss during times of climatic stress reduces transpiration and the associated risk of embolism (Wolfe *et al.*, 2016). Trees that are transpiring during periods of hydraulic stress require adaptations to avoid hydraulic failure, such as deep roots or high wood density, which is often positively correlated with resistance to embolism formation (Hacke *et al.*, 2001). However, higher wood density comes at the expense of growth rate and height gain, which is an important factor in competitive light-limited environments such as tropical forests (Swenson & Enquist, 2007). Although drought avoidance and drought tolerance represent two largely independent strategies, there is significant diversity in species' trait combinations (Markestijn & Poorter, 2009). As a result, the most useful single metric of water deficit tolerance for species within a given size class may be geographical distribution across moisture gradients (e.g. Condit *et al.*, 2013). Given the more challenging hydraulic environment faced by large trees, we expect that at sites subject to predictable periods of water limitation (i.e. dry seasons), or where mild to moderate drought occurs frequently, canopy species should exhibit stronger drought adaptations compared to understory trees. We further expect that, when drought adaptations are insufficient to compensate for the harsher microclimate faced by larger trees, the relative contributions of larger trees to ecosystem-level productivity and biomass should be reduced under more arid conditions.

The greater sensitivity of large trees to drought stress should have important implications for ecosystem-level C cycling and forest feedbacks to climate change, yet this remains poorly understood. Only a couple of studies have quantified the role of tree size in ecosystem-level C cycle drought responses of tropical forests (Bennett *et al.*, 2015), both showing large reductions of live-tree biomass as a result of the more pronounced drought response of larger trees (Nepstad *et al.*, 2007; da Costa *et al.*, 2010). Most ecosystem models do not yet incorporate size-related variation in hydraulic traits, but those that do are better able to reproduce observed forest ecosystem responses to drought (Rowland *et al.*, 2015; Christoffersen *et al.*, 2016). Improved

quantification of C cycle contributions, drought adaptations and drought responses as a function of tree size, will be key to improving our understanding of tropical forest ecosystem responses to spatial and temporal variation in moisture stress.

A series of well-studied moist tropical forest plots spanning a gradient of dry season moisture availability across the isthmus of Panama and subject to droughts during El Niño events provide the opportunity to better understand the C cycle contributions, drought adaptations and drought responses of trees of different sizes (Table 1; e.g. Leigh *et al.*, 1990; Condit *et al.*, 1995, 2000, 2013; Condit, 1998a). In 1981, a 50-ha long-term monitoring plot, the first of the Center for Tropical Forest Science-Forest Global Earth Observatory (Anderson-Teixeira *et al.*, 2015), was established on Barro Colorado Island (Condit, 1998a; Hubbell *et al.*, 1999). Shortly thereafter, the major El Niño event of 1982–83 caused severe dry season drought, resulting in high mortality, particularly among large trees, followed by a rapid rebound in terms of leaf area and forest structure (Leigh *et al.*, 1990; Condit *et al.*, 1995, 1999). Additional sites were established at the drier (Cocoli) and wetter (San Lorenzo) ends of the moisture gradient in 1994 and 1996, respectively (Condit *et al.*, 2000, 2004, 2013). These plots were resurveyed before and after another major El Niño event in 1997–98, which significantly increased mortality only at the driest site, where again larger trees suffered more (Condit *et al.*, 2004). It remains to be quantified how whole-ecosystem C cycling is shaped by trees of different sizes and drought adaptations across this gradient and how these patterns relate to spatial and temporal variation in water availability.

Here, we analyze data from these three sites (Table 1) to test three hypotheses regarding how $C_{ag, live}$, $ANPP_{stem}$ and M are shaped by trees of different sizes and drought adaptations and how these patterns relate to spatial and temporal variation in moisture stress: (1) contributions to $C_{ag, live}$, $ANPP_{stem}$ and M increase with tree size under nondrought conditions, with large trees contributing proportionately less at the drier end of the moisture gradient; (2) community composition is such that drought adaptations (deciduousness, high wood density and water deficit tolerance, a metric based on species distribution in response to moisture amounts) are accentuated in the larger size classes, particularly at the drier end of the gradient, and therefore drought adapted species contribute disproportionately to $C_{ag, live}$, $ANPP_{stem}$ and M ; and (3) focusing on the two instances where the effects of El Niño drought stress were evident through increases in tree mortality (1982–83 El Niño at Barro Colorado Island and 1997–98 El Niño at Cocoli; Condit *et al.*, 1995, 1999), we expect negative impacts to the ecosystem C balance (e.g. elevated mortality and decreased $ANPP_{stem}$) to increase with tree size.

Materials and Methods

Study sites and data

Tree censuses were conducted at three sites spanning a gradient of dry season moisture availability ('moisture' for brevity) in Panama: Cocoli, Barro Colorado Island and San Lorenzo, also

Table 1 Basic information on the three sites spanning the Panama moisture gradient

	Cocoli	Barro Colorado Island	San Lorenzo
Plot information			
Latitude, longitude	8.9877, -79.6166	9.1543, -79.8461	9.2815, -79.974
Size (ha)	4	50 (48.1*)	6 (4.96*)
Census years	1994, 1997, 1998	1981, 1985, 1990, 1995, 2000, 2005, 2010	1996, 1997, 1998, 2009
Focal non-El Niño census period	1994 [†] –1997	1990–1995 [†]	1996 [†] –1997
Plot descriptions	Condit <i>et al.</i> (2000, 2004)	Condit (1998a), Hubbell <i>et al.</i> (1999)	Condit <i>et al.</i> (2000, 2004)
Climate (1995–2010 mean)			
Mean annual temperature (°C)	26.0	27.4	25.6
Mean annual precipitation (mm)	1808	2167	3197
Mean maximum dry season moisture deficit (mm) [‡]	575	514	492
Vegetation			
Stem density (stems \geq 1 cm DBH; ha ⁻¹)	2470	5155	3441
Species richness (stems \geq 1 cm DBH; full plot)	173	323	268
% of canopy species deciduous [§]	42.1	32.2	23.8

Unless otherwise noted, vegetation properties are as calculated in this study for censuses between 1994 and 1996.

*Plot size after relatively young 1–2-ha patches of secondary forest were excluded from these analyses.

[†]Indicates focal census for stem density and biomass calculations.

[‡]Values from Condit *et al.* (2013). Briefly, dry season moisture deficit is calculated as the sum of daily deficit values (D_d ; mm per month), where D_d is the difference between potential evapotranspiration (PET) and precipitation, and the maximum cumulative deficit is averaged across years. To avoid breaking the dry season into separate calendar years, D was calculated for September to July of the following year. Precipitation and PET are interpolated based on local weather stations.

[§]Canopy defined as diameter at breast height (DBH) \geq 30 cm. These values are similar to those reported by Condit *et al.* (2000), but have been updated according to the list of deciduous species used here (Supporting Information Table S1).

known as Sherman (Table 1; Condit, 1998a,b; Hubbell *et al.*, 1999, 2010; Condit *et al.*, 2000). All sites are tropical moist lowland forests with differing proportions of evergreen and deciduous species (Table 1; Condit *et al.*, 2000). Cocoli is on the drier Pacific side of the gradient, and is a secondary forest *c.* 100 yr old (Condit, 1998b). The 50-ha Barro Colorado Island plot is located on a 1500-ha island in Gatun Lake and is primarily old-growth forest that has been undisturbed by humans for over 500 yr (Condit, 1998b). The site with the highest moisture, San Lorenzo, is a mature forest near the Atlantic coast that has been subject to some logging or clearing activity during the last 150 yr (Condit, 1998b). We excluded from the analyses a 1-ha patch of young, secondary forest within San Lorenzo (Condit *et al.*, 2004) and a 1.9-ha patch at Barro Colorado Island (Harms *et al.*, 2001), because these patches of secondary forest differ from the rest of the plot in species composition and are expected to differ in growth and mortality patterns. Plots were censused following a standardized protocol in which all stems \geq 1 cm diameter at breast height (DBH) were mapped, tagged, identified to species, and measured in DBH (1.3 m) or, for all censuses except the first Barro Colorado Island census, above any buttresses or other stem irregularities (Manokaran *et al.*, 1990; Condit, 1998a). Data current as of February 29, 2016 were downloaded from the Center for Tropical Forest Science database (<http://ctfs.si.edu/ctfsrep>).

Three metrics related to drought adaptation were available for the majority of species at these three plots: deciduousness, wood density and a moisture association index (MAI). Deciduous species were defined based on surveys and expert knowledge as those species capable of deciduousness at any site or in any size class (Supporting Information Methods S1; Table S1; Condit *et al.*, 2000). Analyses were conducted both including and

excluding brevideciduous species, which are species that experience a very brief loss of leaves. Wood density values (g cm^{-3}) were obtained from central Panama (for methods see Wright *et al.*, 2010) or from the Center for Tropical Forest Science wood density dataset (<http://ctfs.si.edu/Public/Datasets/CTFSWoodDensity/>). If there was no value at the species level, we used the genus-level mean (used for 16.6% of total species) or the family-level mean (7.1% of total species). At the site level, this corresponded to genus-level values for 7.0%, 8.3% and 15.9% of species and family-level values for 2.3%, 3.8% and 9.5% of species at Cocoli, Barro Colorado Island and San Lorenzo, respectively. These species tended to be rare (in total representing just 2.2% of individuals). If an individual was unidentified or had no available wood density value at any taxonomic level, the mean of all other species at the site was used. Wood density values were lacking for only one rare tree (*Besleria robusta*, $n = 4$). A species-level MAI was assigned to 80% of species based on a study using environmental predictors to model tree distributions in Panama (Condit *et al.*, 2013). The model used eight climatic and soil factors, one of which was dry season moisture deficit, in a hierarchical Gaussian logistic regression to predict species occurrence, and we defined MAI as the species-specific moisture response parameter returned by the model.

Precipitation and temperature data were obtained from local weather stations for each site. Measurements for Barro Colorado Island were taken at 'El Claro', a station established in a clearing *c.* 2 km from the plot in 1972. Data for San Lorenzo were collected from a crane built in 1997 adjacent to the plot, and data gaps were filled using records from Gatun West, a Panama Canal Authority (Autoridad del Canal de Panamá – ACP) station located 5.3 km southeast of San Lorenzo. Cocoli records were

taken from the Parque Natural Metropolitano canopy crane established in 1995 at the northwestern edge of Panama City, and missing values were filled by averaging data from two nearby ACP stations – Albrook Airbase and Balboa Heights, located 4–5 km away. Rainfall measurements from ACP stations were corrected to match plot stations for both Cocoli and San Lorenzo using a linear regression developed by Steve Paton (http://biogeodb.stri.si.edu/physical_monitoring/). At Barro Colorado Island only, soil moisture was sampled from depths of 0–10 cm at 10 sites around the Lutz catchment, and solar radiation was measured by a pyranometer on top of the Lutz tower, close to the meteorological station ‘El Claro.’

Analyses

Our analyses for stem density and total site biomass focused on the census nearest to 1995 (before 1997–98 El Niño), whereas those for growth and mortality focused on census periods that were the closest to overlapping and with no major El Niño events (Cocoli: 1994–1997, Barro Colorado Island: 1990–1995, San Lorenzo: 1996–1997; Table 1).

All analyses were conducted at the stem (ramet) level; i.e. those stems that arose from the same root system or collar were examined individually as opposed to jointly at the tree (genet) level. To account for the fact that individual stems of multi-stemmed individuals were not assigned unique identifiers during censuses, we developed an algorithm to determine the probable alignment of stem IDs from one census to the next (Methods S2). For stems measured at a height other than the standard 1.3 m height of measurement – including 0.98–3.78%, 0.51–1.69% and 1.26–1.36% of stems at Cocoli, Barro Colorado Island and San Lorenzo, respectively – we applied a taper correction to give an equivalent DBH at 1.3 m (Cushman *et al.*, 2014). All tree ferns (*Cyathea* spp.) and strangler figs (*Ficus bullenei*, *F. colubrinae*, *F. costaricana*, *F. citrifolia*, *F. pertusa* and *F. popenoei*) were excluded from these analyses because their growth is not well characterized by trunk diameter. Additional corrections to the data and exclusions of outliers are detailed in Methods S2.

Carbon cycling variables Variables describing ecosystem-level carbon (C) cycling were calculated as follows. Biomass was estimated based on allometries developed by Chave *et al.* (2014). The equation selected was designed for use when tree height measurements are unavailable and instead accounts for diameter–height allometries using an environmental stress parameter (E), which is a function of climatic water deficit, temperature seasonality, and precipitation seasonality. Values for E were extracted from http://chave.ups-tlse.fr/pantropical_allometry.htm and were found to be 0.0748 for Cocoli, 0.0518 for Barro Colorado Island and –0.0565 for San Lorenzo. Biomass was converted to C using the approximation that biomass is 47% C (IPCC, 2006). For comparison, we also estimated biomass using the same equation for all sites; that is, instead of incorporating different E values, all three sites used the allometry designed for ‘moist’ forests (Chave *et al.*, 2005). We found that this allometry resulted in higher carbon estimates for all sites, but did not result in substantive differences

among analyses (Table S2; Fig. S1), and we therefore only reported the results obtained from the Chave *et al.* (2014) allometric equation. For palm trees (*Arecaceae*), biomass was estimated using the family-level equation based on diameter developed by Goodman *et al.* (2013), and was adjusted for log transformation bias using a correction factor (Chave *et al.*, 2005).

Aboveground net primary production of stem biomass C ($\text{ANPP}_{\text{stem}}$; $\text{Mg C ha}^{-1} \text{yr}^{-1}$) was calculated as the sum of annual biomass C growth for stems that were alive at the beginning and end of a census period, plus the biomass C in stems that recruited into the census, all divided by the census interval (following variable definition in Anderson-Teixeira *et al.*, 2016). Woody mortality (M ; $\text{Mg C ha}^{-1} \text{yr}^{-1}$) was calculated as the sum of the aboveground biomass C of all stems that died divided by the census interval, with biomass C estimates based on DBH measurements from the most recent census before death. Net biomass C change was calculated as $\text{ANPP}_{\text{stem}} - M$. Initial $C_{\text{ag, live}}$ was defined as the sum of live biomass C for stems at the initial census for each census period. For the first census period on Barro Colorado Island, a correction was applied to estimate $\text{ANPP}_{\text{stem}}$, M , and net biomass change because all measurements were made at 1.3 m, including around buttresses or other stem abnormalities, for this one census (Table S3; Methods S2). These values were determined for all plants ≥ 1 cm DBH and for the following diameter classes: 1–10, 10–50, and ≥ 50 cm (Table S4).

Size-related variation In order to analyze how the variables of interest varied with stem size, stems were grouped into 23 approximately log-even bins based on their initial diameter. Stem density ($n \text{ ha}^{-1}$), $C_{\text{ag, live}}$, $\text{ANPP}_{\text{stem}}$ and M per cm DBH were calculated for each size class, as was the mean initial diameter (\bar{D}_0 ; i.e. diameter measured at the first census of each interval). For all variables, we fitted the following function to \log_e -transformed data:

$$y = a\bar{D}_0^b \exp^{c\bar{D}_0} \quad \text{Eqn 1}$$

Here, a , b and c are fitted parameters, where $c = 0$ gives a power function and negative or positive values of c give hump- or U-shaped fits, respectively. Ninety-five percent confidence intervals were calculated by randomly sampling 10×10 m subplots for each variable using 1000 bootstrap replicates. We also quantified size-related variation in several of the underlying variables: individual biomass C, diameter growth, individual biomass C growth and stem mortality (Methods S3; Fig. S2).

The variation of interspecific functional trait distributions among stem size classes also was analyzed. Mean deciduousness, wood density and MAI were calculated for each of eight approximately log-even size classes and for the community as a whole. A linear-log function was then fitted using linear least squares regression to \log_e -transformed values of DBH. Weighted means for deciduousness, wood density and MAI were calculated as $\sum T_i(C_i/C_{\text{tot}})$, where T_i is the functional trait value attributed to each individual stem based on its species identity and C_i and C_{tot} are $C_{\text{ag, live}}$, $\text{ANPP}_{\text{stem}}$ or M of the individual or entire community, respectively.

Results

C cycling and tree size across the moisture gradient

Contrary to expectations, we reject the first component of Hypothesis 1, that $C_{ag, live}$, $ANPP_{stem}$ and M increase with tree size under nondrought conditions, and instead find that these variables peaked below 50 cm DBH (Fig. 1b–d). When considering ecosystem-level attributes as a function of DBH on a linear scale (i.e. per cm increase in DBH; Fig. 1), stem density declined sharply with DBH with an accelerating decline at all sites; that is, the fit parameters b and c (Eqn 1) were consistently negative (Fig. 1a; all $P < 0.001$; Table S5). Because individual biomass C increases steeply with DBH (Fig. S2a; Table S5), $C_{ag, live}$ increased with DBH across the lower end of the size range (Fig. 1b; all $b > 0.67$; all $P < 0.001$), peaking between mid and 50 cm DBH, and declining in the largest size classes (all $c < 0$; all $P < 0.001$). Diameter growth rate and individual biomass C growth rates both increased monotonically with DBH (Fig. S2b,c; Table S5). $ANPP_{stem}$ displayed hump-shaped relationships with DBH at Barro Colorado Island and San Lorenzo (Fig. 1c; both $b > 0.14$, all $c < -0.02$, both $P < 0.04$), but there was no significant trend at Cocoli ($P = 0.44$). Stem mortality rate decreased with DBH (Fig. S2d; Table S5), whereas M increased across most of the size range at all sites (Fig. 1d, all $b > 0.27$; all $P \leq 0.03$), before declining at $DBH > 50$ cm at Barro Colorado Island and San Lorenzo (both $c < -0.01$, both $P \leq 0.001$).

Expressed in terms of three broad size classes (1–10, 10–50 and > 50 cm DBH), ecosystem-level C cycling ($C_{ag, live}$, $ANPP_{stem}$, M) was dominated by large and mid-sized stems (Fig. 1; Table S4). Specifically, across sites and censuses, stems ≥ 50 cm had the lowest stem densities (mean of 32 stems ha^{-1} ; range: 30–38), but still contributed the most to C cycling, representing on average 45% of $ANPP_{stem}$ (range: 29–64%), 49% of M (range: 19–63%) and 59% of $C_{ag, live}$ (range: 49–68%; Table S4). Stems 10–50 cm DBH had an average stem density of 400 stems ha^{-1} (range: 244–493) and contributed almost as much C as large stems, comprising on average 44% of $ANPP_{stem}$ (range: 29–55%), 45% of M (range: 33–72%) and 37% of $C_{ag, live}$ (range: 30–47; Table S4). By contrast, the smallest stems (< 10 cm DBH) had a mean stem density of 4020 stems ha^{-1} (range: 2282–5284), and contributed least to C cycling, representing only an average 11% of $ANPP_{stem}$ (range: 6–16%), 6% of M (range: 3–9%) and 4% of $C_{ag, live}$ (range: 2–5%; Table S4).

Across the gradient, there were no consistent trends in ecosystem-level C cycling or its partitioning across size classes. Specifically, at the ecosystem level, $C_{ag, live}$ tended to increase with decreasing dry season intensity, but with overlapping 95% CIs (Tables 2, S4) – a trend that is potentially confounded by the fact that the driest site (Cocoli) is a secondary forest. This trend was less pronounced when allometries from Chave *et al.* (2005) were used, with San Lorenzo and Barro Colorado Island displaying similar values (Table S2). M also tended to increase with decreasing dry-season intensity, whereas $ANPP_{stem}$ showed no consistent

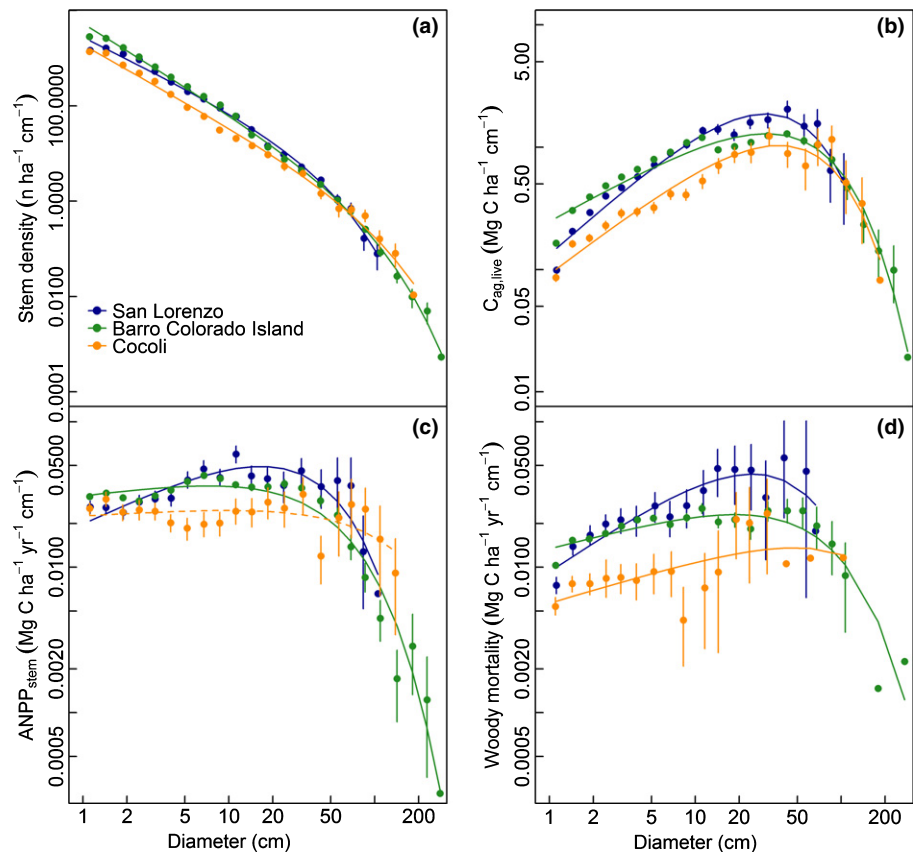


Fig. 1 Size-related variation in (a) stem density, (b) aboveground live biomass carbon ($C_{ag, live}$), (c) aboveground woody productivity ($ANPP_{stem}$) and (d) woody mortality (M) at all three sites during the focal non-El Niño census periods (Table 1). Totals for each size bin are divided by the width of the size bin (cm) such that relationships depict how these variables change with diameter on a linear scale. Dashed lines indicate a nonsignificant trend. Fit parameters and statistics are given in Supporting Information Table S5. Vertical lines depict 95% confidence intervals based on bootstrapping over subplots.

Table 2 Ecosystem-level carbon (C) variables including live biomass C ($C_{ag, live}$), woody productivity ($ANPP_{stem}$), woody mortality (M) and net biomass C change for all three sites during non-El Niño census periods

		$C_{ag, live}$ (95% CIs) (Mg C ha ⁻¹)	$ANPP_{stem}$ (95% CIs) (Mg C ha ⁻¹ yr ⁻¹)	M (95% CIs) (Mg C ha ⁻¹ yr ⁻¹)	Net biomass C change (95% CIs) (Mg C ha ⁻¹ yr ⁻¹)
Cocoli	1994*–97	120 (105,132)	3.07 (2.63, 3.52)	1.18 (0.61, 1.99)	1.89 (0.90, 2.72)
Barro Colorado Island	1990–95*	136 (129,143)	2.76 (2.62, 2.91)	2.43 (2.04, 2.85)	0.32 (–0.14, 0.70)
	Non-El Niño mean	136	3.20	2.63	0.57
San Lorenzo	1996*–97	144 (130,157)	3.44 (2.98, 3.95)	2.83 (1.89, 3.95)	0.61 (–0.59, 1.75)
	Non-El Niño mean	146	2.78	2.94	–0.16

Shown are records for our focal census periods (Table 1) and the mean for all non-El Niño census periods.

*Indicates year for which $C_{ag, live}$ is reported.

trends across the gradient (Table 2). Net biomass C change was significantly positive in Cocoli, the secondary forest, and was not significantly different from zero at the other two sites. For all of these variables, there was little evidence of systematic differences in the relative contributions of trees of different sizes across the moisture gradient (Figs 1, S2; Tables S4, S5); thus, we reject the second component of Hypothesis 1, that large trees contribute proportionately less to C cycling at the drier end of the moisture gradient.

Tree size and drought adaptations

The dominance of deciduous species increased with DBH at all sites, particularly at the drier sites (Fig. 2a,b; Table S6), in

concordance with Hypothesis 2. Specifically, the fractional abundance of deciduous species increased significantly with DBH at all sites, regardless of whether brevideciduous species were classified as evergreen or deciduous (all $P \leq 0.01$). As expected, the steepness of the slope of this relationship increased with climatic water deficit; that is, whereas the three sites had similarly low fractions of deciduous species in the small size classes, the deciduous fraction of larger trees increased from the wettest to the driest site (Fig. 2a). This resulted in weighted mean deciduousness being greater for $C_{ag, live}$, $ANPP_{stem}$ and M than for stem density, indicating that relative to their abundance, deciduous species contributed disproportionately to biomass C and changes therein (Fig. 2b). Although total fractions of deciduous species were similar across sites (largely due to the high abundance of evergreen

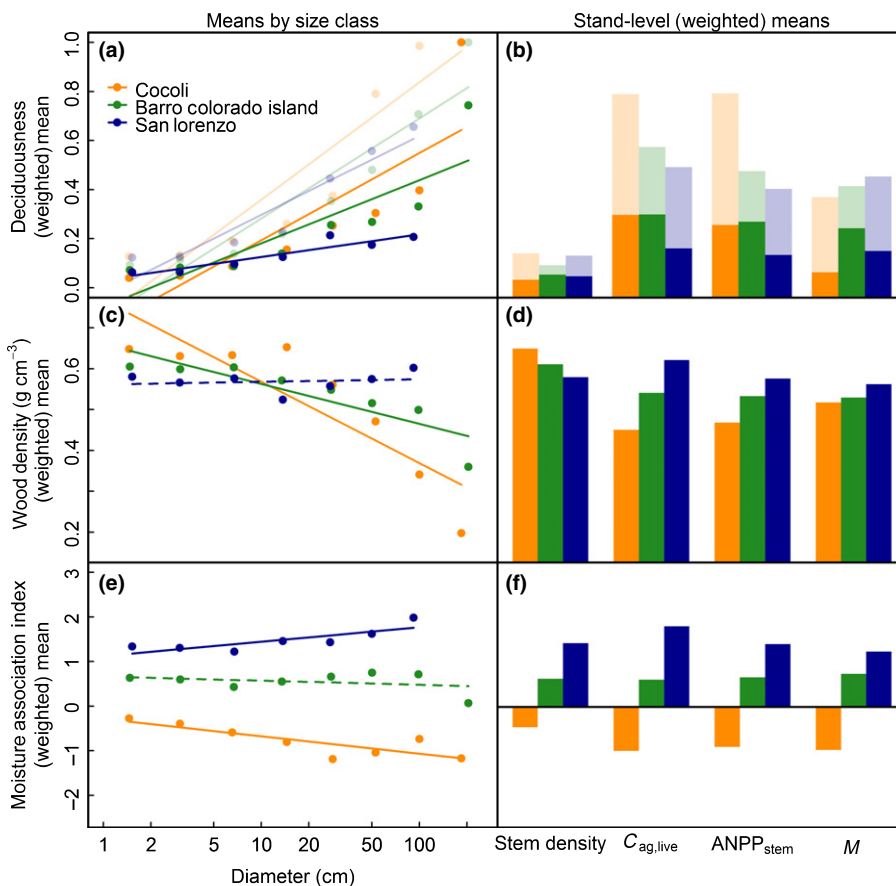


Fig. 2 Deciduousness (a, b), wood density (c, d) and moisture association index (MAI; e, f) averaged by size class (a, c, e) and as means weighted according to stems' contributions to total stem density, live biomass carbon (C) ($C_{ag, live}$), woody productivity ($ANPP_{stem}$) and woody mortality (M) (b, d, f). For deciduousness, results are presented counting brevideciduous species as evergreen (solid colors) or deciduous (pale colors), with 0 indicating nondeciduous and 1 indicating deciduous. For MAI, negative values represent species associated with drier climates and positive values correspond to species associated with wetter climates (Condit *et al.*, 2013). Dashed lines indicate nonsignificant trends. Results apply to the focal censuses identified in Table 1.

stems in the small size classes; Table 1; Fig. 2a,b), the contributions of deciduous species to $C_{\text{ag, live}}$ and $\text{ANPP}_{\text{stem}}$ increased with climatic water deficit, indicating that the disproportionate influence of deciduous species on C cycling was greatest at the driest site (Fig. 2b).

As with deciduousness, differences in wood density were accentuated in the larger size classes and at drier sites (Fig. 2c); however, contrary to Hypothesis 2, the larger trees at drier sites had lower wood density. Specifically, mean wood density decreased with DBH at the two drier sites (both $P < 0.004$), but not at San Lorenzo ($P = 0.71$; Fig. 2c; Table S6). Species with higher wood density were more abundant at Cocoli than the wetter sites across most of the size spectrum, but this pattern reversed in the largest size classes (Fig. 2c). At Cocoli and Barro Colorado Island, species with low wood density contributed disproportionately to C cycling, as illustrated by lower weighted mean wood density for $C_{\text{ag, live}}$, $\text{ANPP}_{\text{stem}}$ and M than for stem density (Fig. 2d). Furthermore, although community-wide mean wood density decreased with increasing moisture across the gradient, weighted mean wood density increased with moisture for $C_{\text{ag, live}}$, $\text{ANPP}_{\text{stem}}$ and M ; that is, the relative importance of low wood density species in the larger size classes increased with climatic water deficit (Fig. 2d). The decrease in wood density with stem size was driven primarily by deciduous canopy species with low wood density, particularly at Cocoli, where exclusion of deciduous species made this trend disappear ($P = 0.99$).

As expected, and consistent with how MAI is defined, the mean MAI value varied across the moisture gradient, with the greater abundance of xerophytic species at Cocoli and of mesophytic species at San Lorenzo (Fig. 2e). Interestingly, differences were more pronounced in the larger size classes; mean MAI decreased with DBH at Cocoli ($P = 0.009$), did not vary significantly with DBH at Barro Colorado Island ($P = 0.45$) and increased with DBH at San Lorenzo ($P = 0.03$; Fig. 2e; Table S6). As with deciduousness and wood density, the MAIs associated with larger trees tended to be disproportionately influential to C cycling, such that weighted mean MAI for $C_{\text{ag, live}}$, M , $\text{ANPP}_{\text{stem}}$ varied more markedly across the moisture gradient than did mean MAI based on abundance.

Responses to El Niño events

The El Niño events disproportionately affected the largest trees at both Barro Colorado Island and Cocoli, as predicted in Hypothesis 3. At Barro Colorado Island, the 1982–83 El Niño was characterized by anomalously warm temperatures lasting from May 1982 to June 1983 (peak mean monthly temperature of 29.30°C in April 1983 was the highest on record from 1980 to 2010), low November–April precipitation (289 mm in 1982–83 compared to a 1980–2010 mean of 1041 mm) and the lowest soil moisture on record from 1980 to 2010 (27.1% water by wet weight compared to a 1980–2010 mean of 38.9%). The drought stress resulted in high tree mortality (Condit *et al.*, 1995), such that M (4.86 Mg C ha⁻¹ yr⁻¹) was almost double the mean value for census periods lacking a major El Niño event

(2.63 Mg C ha⁻¹ yr⁻¹; Table S4). Increases in M above the non-El Niño mean were particularly pronounced for larger stems, with stems ≥ 50 cm DBH responsible for 63% of total M (3.06 Mg C ha⁻¹ yr⁻¹; Fig. 3e; Tables 3, S4). $\text{ANPP}_{\text{stem}}$ was also elevated during the 1981–1985 census period, effectively compensating for the high M (net biomass C change = 0.70 Mg C ha⁻¹ yr⁻¹; Fig. 3a,c; Tables 3, S4). The largest stems (≥ 50 cm) were the only size class to have a negative net biomass C change value (−0.24 Mg C ha⁻¹ yr⁻¹; Tables 3, S4). It should be noted that although we sought to correct for the changes in measurement height protocol between the 1981 and 1985 Barro Colorado Island censuses (Methods S2), values for this census period are less accurate than the others reported here.

At Cocoli, the 1997–98 El Niño resulted in elevated November–April temperature (26.9°C, compared to mean of 26.2°C for 1995–2010 non-El Niño years) and decreased November–April rainfall (347 mm; 1995–2010 non-El Niño mean: 550 mm). $\text{ANPP}_{\text{stem}}$ decreased relative to the preceding non-El Niño period whereas M increased, resulting in a net decline in $C_{\text{ag, live}}$ (Fig. 3; Table 3). Specifically, $\text{ANPP}_{\text{stem}}$ declined 26% (from 3.07 to 2.28 Mg C ha⁻¹ yr⁻¹; Table S4). This was driven by the larger size classes (Fig. 3d): although $\text{ANPP}_{\text{stem}}$ of stems ≥ 50 cm DBH declined, $\text{ANPP}_{\text{stem}}$ of stems < 10 cm increased (Table 3). Meanwhile, M increased 170% (from 1.18 to 3.18 Mg C ha⁻¹ yr⁻¹), with the largest contribution (63%) coming from stems ≥ 50 cm DBH (Table 2; Fig. 3f). Total $C_{\text{ag, live}}$ declined overall, increasing for smaller stems while decreasing for larger stems (Fig. 3b; Tables 3, S4).

Discussion

Across three large forest plots in Panama, ecosystem-level carbon (C) cycling was dominated by mid- to large-sized trees, with contributions per unit diameter at breast height (DBH) typically peaking in the 10–50 cm DBH range and trees ≥ 50 cm DBH representing an average of 59% of live aboveground biomass ($C_{\text{ag, live}}$) and contributing somewhat less to changes therein (45% woody productivity, $\text{ANPP}_{\text{stem}}$, and 49% woody mortality, M ; Fig. 1, Table S4), despite their low stem density (0.8%, on average; Table S4). We found little difference in the relative C cycle contributions of large vs small trees across the moisture gradient (Fig. 1), indicating that the observed differences in community composition were sufficient to compensate for any differential biophysical challenges faced by larger trees in drier climates. Indeed, larger stems showed evidence of stronger drought adaptations, having higher fractions of deciduous species and more pronounced sorting across a geographical moisture gradient (Fig. 2; Condit *et al.*, 2000, 2013). Despite these adaptations, in association with El Niño drought stress at Barro Colorado Island in 1982–83 and at Cocoli in 1997–98, larger trees suffered greater increases in mortality, dominating ecosystem-level C cycle responses (Fig. 3e,f; Table 3). Thus, it is generally the mid-sized to large trees – those with at least some chance of being in an exposed canopy position (Muller-Landau *et al.*, 2006a) – that display the most pronounced drought adaptations, suffer most under drought (see also Condit *et al.*, 1995, 2004; Bennett *et al.*,

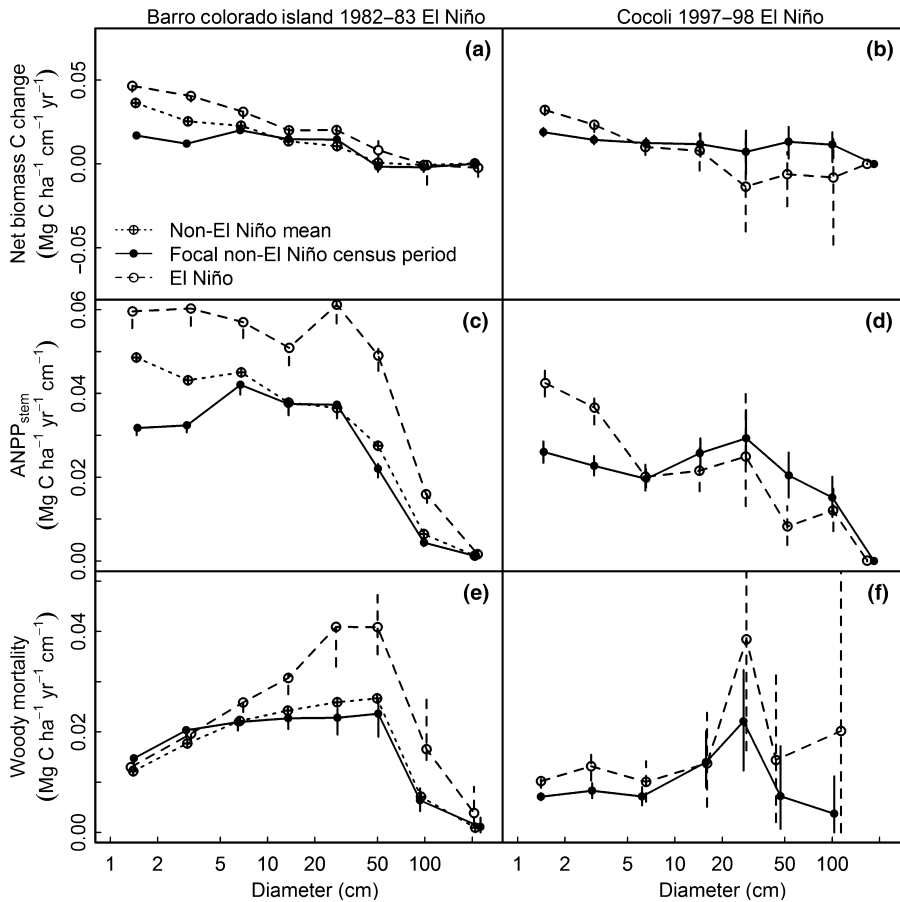


Fig. 3 Comparison of (a, b) net biomass carbon (C) change, (c, d) woody productivity ($ANPP_{stem}$), and (e, f) woody mortality (M) by size class in El Niño and non-El Niño years at Barro Colorado Island (1982–83 El Niño) and Cocoli (1997–98 El Niño). Non-El Niño means include all census periods that did not include a major El Niño event (see Table 1). Stems were divided into eight log-even bins and the total value for each size bin was divided by the width of the size bin (cm) to depict how each variable changes with diameter on a linear scale. Vertical lines depict 95% confidence intervals based on bootstrapping over subplots.

Table 3 El Niño-driven changes in woody productivity ($ANPP_{stem}$), woody mortality (M) and net biomass carbon (C) change by size class, with change expressed relative to non-El Niño census period means (Table 1 and Supporting Information Table S4).

Event	Size class (cm)	$ANPP_{stem}$	M	Net biomass C change
Barro Colorado Island 1982–83 El Niño	1–10	+0.11	+0.03	+0.09
	10–50	+0.84	+0.54	+0.30
	≥50	+1.40	+1.65	–0.26
	All (≥1)	+2.35	+2.22	+0.13
Cocoli 1997–98 El Niño	1–10	+0.06	+0.03	+0.02
	10–50	–0.09	+0.44	–0.53
	≥50	–0.76	+1.53	–2.28
	All (≥1)	–0.79	+2.00	–2.79

All variables have units of $Mg\ C\ ha^{-1}\ yr^{-1}$.

2015), and most strongly mediate forest C cycle responses to hydraulic stress.

One novel finding of this study is that – contrary to Hypothesis 1 – aboveground biomass and C cycling are not dominated by the largest trees, but tend rather to peak at intermediate stem diameters (Figs 1b–d, S3). Specifically, when C cycle contributions were expressed as a linear function of DBH – consistent with previous literature on size scaling in forests (e.g. Muller-Landau *et al.*, 2006b; West *et al.*, 2009; Lutz *et al.*, 2012)

– $C_{ag, live}$ peaked at 27–50 cm DBH, whereas maximum contributions to $ANPP_{stem}$ and M occurred at < 50 cm DBH. It is important to note that interpretations of C cycle contributions as a function of DBH are influenced by the way that size bins are defined. When DBH was expressed on a logarithmic scale – i.e. size bin width increasing with DBH – C cycle contributions increased continuously with DBH across most of the size spectrum (Fig. S3). Nevertheless, under either approach, it was not the largest trees that contributed most to biomass and C cycling; rather, their rarity made their contributions less than those of intermediate-sized stems. By contrast, although stems < 10 cm DBH contributed relatively little to live aboveground biomass at these sites ($\leq 5.2\%$), their contributions to $ANPP_{stem}$ and M were more significant (ranging up to 15.9% and 8.7%, respectively). It is particularly striking that at Barro Colorado Island and Cocoli, $ANPP_{stem}$ per cm DBH was similar across all size classes below $c. 50$ cm DBH and that contributions to $ANPP_{stem}$ declined above this threshold (Fig. 1c). The relatively high contributions of small stems to $ANPP_{stem}$ and M reflect high biomass turnover rates, driven by relatively high stem mortality (Fig. S2d) and mass-specific growth rates (i.e. individual net biomass C change/ $C_{ag, live}$; Fig. S2a,b). Although the contributions of small stems should not be ignored, it is the mid- to large-sized trees that dominate aboveground C cycling (Fig. 1; Table S4) and should be most important in driving tropical forest C cycle responses to climatic variation in space and time.

Contrary to our first hypothesis, we found little evidence of systematic, directional differences in the C cycle contributions of trees of different sizes across the moisture gradient (Fig. 1; Tables S4, S5). Based on the observed greater drought sensitivity of larger trees (Bennett *et al.*, 2015), we may have expected relatively smaller C cycle contributions of larger trees under drier conditions (Hypothesis 1). However, across this modest moisture gradient, the drought adaptations associated with larger trees in drier climates were sufficient to compensate for any stronger hydraulic stress experienced by these trees because of their canopy position. Of course, extending into far drier climates, large trees – and their carbon cycle contributions – completely disappear.

Species' drought adaptations varied with stem size (Fig. 2). The wettest site and understories at all sites were dominated by evergreen species with relatively high wood density, whereas the dominance of deciduous species increased, and mean wood density decreased, with increasing tree size and dry season intensity (Fig. 2a). These patterns are largely consistent with our second hypothesis and with the principle that larger, taller trees face more challenging hydraulic constraints than do their understory counterparts. Canopy trees are exposed to higher solar radiation and leaf-to-air vapor pressure deficit, which may make it difficult to simultaneously maintain hydraulic safety, regulate leaf temperature, and maintain a positive C balance during dry conditions (Roberts *et al.*, 1990; Nepstad *et al.*, 2007; Bennett *et al.*, 2015). Dry season deciduousness is one drought adaptation strategy that allows trees to avoid these stressors (Markesteijn & Poorter, 2009), and our results (Fig. 2) – along with previous findings (Frankie *et al.*, 1974; Wright, 1991; Condit *et al.*, 2000) – make it apparent that this strategy is increasingly favored under drier conditions and for larger trees, supporting Hypothesis 2. In fact, the magnitude of the observed increase in deciduousness with stem size (Fig. 2a) is likely underestimated in this study because individual species are often deciduous as big trees but not as juveniles (Condit *et al.*, 2000). Size trends in deciduousness (Fig. 2a) and C cycle contributions (Fig. 1) combined such that deciduous species contributed disproportionately to forest C cycling relative to their abundance in the community (Fig. 2b), particularly at the two drier sites. Thus, capturing the observed size trend in deciduousness will be essential to accurately modeling C cycling and its seasonality in semi-deciduous tropical forests.

Counterintuitive to the principle that larger trees require stronger drought adaptations (Hypothesis 2) is the fact that wood density declined with stem size at the two drier sites (Fig. 2c). All else being equal, we would expect that trees facing higher water deficits would have higher wood density; however, Panamanian tree species display a wide variety of hydraulic strategies. Low wood density species can be strongly drought-adapted if deciduous, and there was no association between wood density and moisture association index (MAI) among the species included in this analysis ($R^2 = 0.002$; $P = 0.40$). Thus, we interpret the lower average wood density of large individuals (Fig. 2c) as being driven primarily by the facts that low wood density trees can achieve the same strength at lower costs by investing in thicker trunks (Larjavaara & Muller-Landau, 2010) and that, all else being equal,

lower wood density species have faster diameter growth and therefore can reach large diameter faster than high wood-density species. The latter may explain the pronounced dominance of low wood density, mostly deciduous species in the largest size classes at Cocoli, which is a secondary forest (Fig. 2); however, this trend was not observed at San Lorenzo despite its history of selective logging, which has been shown to favor low wood density stands (Carreño-Rocabado *et al.*, 2012). At the two drier sites, declines in wood density with stem size (Fig. 2c) combined with size trends in C cycle contributions (Fig. 1) such that the weighted average wood density of stems contributing to C cycling was consistently lower than community-wide wood density means (Fig. 2d). For forests such as these, models or analyses assuming that community mean wood densities apply across size classes may overestimate biomass, ANPP_{stem} and M .

A suite of hydraulic traits, including but by no means limited to deciduousness and wood density, shape species' overall water deficit tolerance and distribution across geographic gradients, as reflected in our MAI (Condit *et al.*, 2013). This metric is not suitable for direct comparison of drought tolerance across size classes because understory and canopy species are subject to different microclimates. However, consistent with Hypothesis 2, larger trees display stronger geographical sorting across the moisture gradient (Fig. 2e). This suggests that water stress plays a stronger role in shaping their geographical distributions than those of understory species, which experience a more buffered microclimate. Moreover, these results indicate that species associating more strongly with one end of the geographical moisture gradient contribute more to C cycling (Fig. 2f), primarily because of their larger size.

Although the relative C cycle contributions of trees of different sizes did not vary across the moisture gradient, their responses to the El Niño drought events differed. For the El Niño droughts at both Barro Colorado Island (1982–83) and Cocoli (1997–98), the larger trees were more strongly impacted in terms of mortality (Fig. 3; Table S4; Condit *et al.*, 1995, 1999, 2004; Bennett *et al.*, 2015). Consistent with our third hypothesis, the implication for the C balance was, in both cases, a large increase (*c.* $2 \text{ Mg C ha}^{-1} \text{ yr}^{-1}$) in woody mortality, driven by the disproportionate importance of larger trees (Fig. 3; Table 3). Growth responses differed between these two events. At Cocoli, consistent with Hypothesis 3, the 1997–98 El Niño reduced growth in the larger size classes and increased growth in the smaller size classes, resulting in net declines in ANPP_{stem} and $C_{\text{ag, live}}$ (Fig. 3; Table 3). By contrast, high woody mortality associated with the 1982–83 El Niño at Barro Colorado Island appears to have been compensated for by elevated ANPP_{stem} during the same census period (Figs 3; Table 3); this was perhaps driven by competitive release or by positive El Niño growth responses of some species, likely due to the alleviation of light limitation by reduced cloud cover (Graham *et al.*, 2003). In all cases, despite the fact that they did not dominate aboveground C cycling during non-El Niño conditions, it was the response of the larger trees that drove ecosystem-level responses to the El Niño events (Table 3).

Here, we elucidated how spatial and temporal variation in water deficit interact with tree size to shape C cycling in

Panamanian tropical forests, findings that can yield insight into the likely climate change responses of these and other tropical forests. Panamanian forests are adapted to regular dry seasons and moderate droughts, and – in cases where we have data – have shown high resilience to the major El Niño events of 1982–83 and 1997–98 in terms of forest structure and C cycling (Fig. 3c; Leigh *et al.*, 1990; Condit *et al.*, 2004). Thus, moderate climate-change associated droughts are unlikely to dramatically alter forest structure and function. Patterns across the moisture gradient suggest that a gradual drying trend – as may be expected if temperature increases are not accompanied by significant increases in precipitation – would likely result in shifts in community composition, with increasing prevalence of drought-adapted (e.g. deciduous) species, particularly in the larger size classes (Fig. 2). However, to the extent that species compositional changes keep pace with climate change, major changes in C cycling – or size trends therein – may be unlikely across the range of climatic water deficit examined here (Fig. 1). By contrast, a rapid increase in the frequency or intensity of severe El Niño droughts could have substantial impacts on forest size structure and C cycling. Because severe El Niño events disproportionately impact the larger – and commonly older – trees, they stand to have both substantive impacts on the C cycle and relatively long-lasting impacts on forest structure. Thus, if climate change increases severe droughts beyond what these forests have experienced historically, there is potential for eventual deterioration of forest resilience. Better understanding of the factors that confer resilience and vulnerability of mid- to large-sized trees to drought will therefore be particularly important for predicting tropical forest responses to climate change.

Acknowledgements

We gratefully acknowledge the many people who contributed to the forest census data used here. Thanks to Rolando Perez and Steve Paton for information on deciduousness and climate, respectively. The analyses presented here were funded by a Smithsonian Competitive Grants Program for Science to K.J.A-T. The forest dynamics research was made possible by National Science Foundation grants to S.P.H.: DEB-0640386, DEB-0425651, DEB-0346488, DEB-0129874, DEB-00753102, DEB-9909347, DEB-9615226, DEB-9615226, DEB-9405933, DEB-9221033, DEB-9100058, DEB-8906869, DEB-8605042, DEB-8206992, DEB-7922197, support from the Center for Tropical Forest Science, the Smithsonian Tropical Research Institute, the John D. and Catherine T. MacArthur Foundation, the Mellon Foundation, the Small World Institute Fund, and numerous private individuals. Some climate data were obtained from the Meteorology and Hydrology Branch, Panama Canal Authority, Republic of Panama.

Author contributions

V.M. and K.J.A-T. designed the research with input from coauthors; R.C., S.P.H. and S.J.W. collected forest census and trait data; V.M. carried out data analysis and interpretation with

assistance from K.J.A-T., A.J.T., E.B.G-A., V.H., H.C.M-L., S.J.W. and R.C.; and V.M. and K.J.A-T. wrote the manuscript, which was reviewed by all coauthors.

References

- Anderegg WRL, Schwalm C, Biondi F, Camarero JJ, Koch G, Litvak M, Ogle K, Shaw JD, Shevliakova E, Williams AP *et al.* 2015. Pervasive drought legacies in forest ecosystems and their implications for carbon cycle models. *Science* 349: 528–532.
- Anderson-Teixeira KJ, Davies SJ, Bennett AC, Gonzalez-Akre EB, Muller-Landau HC, Joseph Wright S, Abu Salim K, Almeyda Zambrano AM, Alonso A, Baltzer JL *et al.* 2015. CTFS-ForestGEO: a worldwide network monitoring forests in an era of global change. *Global Change Biology* 21: 528–549.
- Anderson-Teixeira KJ, Wang MMH, McGarvey JC, LeBauer DS. 2016. Carbon dynamics of mature and regrowth tropical forests derived from a pantropical database (TropForC-db). *Global Change Biology* 22: 1690–1709.
- Bastin J-F, Barbier N, Réjou-Méchain M, Fayolle A, Gourlet-Fleury S, Maniatis D, de Haulleville T, Baya F, Beeckman H, Beina D *et al.* 2015. Seeing Central African forests through their largest trees. *Scientific Reports* 5: 13 156.
- Beer C, Reichstein M, Tomelleri E, Ciais P, Jung M, Carvalhais N, Rödenbeck C, Arain MA, Baldocchi D, Bonan GB *et al.* 2010. Terrestrial gross carbon dioxide uptake: global distribution and covariation with climate. *Science* 329: 834–838.
- Bennett AC, McDowell NG, Allen CD, Anderson-Teixeira KJ. 2015. Larger trees suffer most during drought in forests worldwide. *Nature Plants* 1: 15139.
- Carreño-Rocabado G, Peña-Claros M, Bongers F, Alarcón A, Licona J-C, Poorter L. 2012. Effects of disturbance intensity on species and functional diversity in a tropical forest. *Journal of Ecology* 100: 1453–1463.
- Chave J, Andalo C, Brown S, Cairns MA, Chambers JQ, Eamus D, Fölster H, Fromard F, Higuchi N, Kira T *et al.* 2005. Tree allometry and improved estimation of carbon stocks and balance in tropical forests. *Oecologia* 145: 87–99.
- Chave J, Réjou-Méchain M, Búrquez A, Chidumayo E, Colgan MS, Delitti WBC, Duque A, Eid T, Fearnside PM, Goodman RC *et al.* 2014. Improved allometric models to estimate the aboveground biomass of tropical trees. *Global Change Biology* 20: 3177–3190.
- Christoffersen BO, Gloor M, Fauset S, Fyllas NM, Galbraith DR, Baker TR, Kruijt B, Rowland L, Fisher RA, Binks OJ *et al.* 2016. Linking hydraulic traits to tropical forest function in a size-structured and trait-driven model (TFS v. 1-Hydro). *Geoscientific Model Development* 9: 4227–4255.
- Condit R. 1998a. *Tropical forest census plots – methods and results from Barro Colorado Island, Panama and a comparison with other plots*. Berlin, Germany and Georgetown, TX, USA: Springer and R.G. Landes.
- Condit R. 1998b. Ecological implications of changes in drought patterns: shifts in forest composition in Panama. *Climatic Change* 39: 413–427.
- Condit R, Aguilar S, Hernandez A, Perez R, Lao S, Angehr G, Hubbell SP, Foster RB. 2004. Tropical forest dynamics across a rainfall gradient and the impact of an El Niño dry season. *Journal of Tropical Ecology* 20: 51–72.
- Condit R, Ashton PS, Manokaran N, LaFrankie JV, Hubbell SP, Foster RB. 1999. Dynamics of the forest communities at Pasoh and Barro Colorado: comparing two 50-ha plots. *Philosophical Transactions of the Royal Society B* 354: 1739–1748.
- Condit R, Engelbrecht BMJ, Pino D, Pérez R, Turner BL. 2013. Species distributions in response to individual soil nutrients and seasonal drought across a community of tropical trees. *Proceedings of the National Academy of Sciences, USA* 110: 5064–5068.
- Condit R, Hubbell SP, Foster RB. 1995. Mortality rates of 205 neotropical tree and shrub species and the impact of a severe drought. *Ecological Monographs* 65: 419–439.
- Condit R, Watts K, Bohlman SA, Pérez R, Foster RB, Hubbell SP. 2000. Quantifying the deciduousness of tropical forest canopies under varying climates. *Journal of Vegetation Science* 11: 649–658.
- Coomes D, Duncan R, Allen R, Truscott J. 2003. Disturbances prevent stem size-density distributions in natural forests from following scaling relationships. *Ecology Letters* 6: 980–989.

- Corlett RT. 2016. The impacts of droughts in tropical forests. *Trends in Plant Science* 21: 584–593.
- da Costa ACL, Galbraith D, Almeida S, Portela BTT, da Costa M, de Athaydes Silva J Jr, Braga AP, de Gonçalves PHL, de Oliveira AA, Fisher R *et al.* 2010. Effect of 7 yr of experimental drought on vegetation dynamics and biomass storage of an eastern Amazonian rainforest. *New Phytologist* 187: 579–591.
- Cushman KC, Muller-Landau HC, Condit RS, Hubbell SP. 2014. Improving estimates of biomass change in buttressed trees using tree taper models. *Methods in Ecology and Evolution* 5: 573–582.
- Enquist BJ, West GB, Brown JH. 2009. Extensions and evaluations of a general quantitative theory of forest structure and dynamics. *Proceedings of the National Academy of Sciences, USA* 106: 7046–7051.
- Fauset S, Johnson MO, Gloor M, Baker TR, Monteagudo MA, Brienen RJW, Feldpausch TR, Lopez-Gonzalez G, Malhi Y, ter Steege H *et al.* 2015. Hyperdominance in Amazonian forest carbon cycling. *Nature Communications* 6: 6857.
- Frankie GW, Baker HG, Opler PA. 1974. Comparative phenological studies of trees in tropical wet and dry forests in the lowlands of Costa Rica. *Journal of Ecology* 62: 881–919.
- Goodman RC, Phillips OL, del Castillo Torres D, Freitas L, Cortese ST, Monteagudo A, Baker TR. 2013. Amazon palm biomass and allometry. *Forest Ecology and Management* 310: 994–1004.
- Graham EA, Mulkey SS, Kitajima K, Phillips NG, Wright SJ. 2003. Cloud cover limits net CO₂ uptake and growth of a rainforest tree during tropical rainy seasons. *Proceedings of the National Academy of Sciences, USA* 100: 572–576.
- Hacke UG, Sperry JS, Pockman WT, Davis SD, McCulloh KA. 2001. Trends in wood density and structure are linked to prevention of xylem implosion by negative pressure. *Oecologia* 126: 457–461.
- Harms KE, Condit R, Hubbell SP, Foster RB. 2001. Habitat associations of trees and shrubs in a 50-ha neotropical forest plot. *Journal of Ecology* 89: 947–959.
- Hubbell SP, Condit RS, Foster RB. 2010. Barro Colorado forest census plot data. [WWW document] URL <https://ctfs.arnarb.harvard.edu/webatlas/dataset/bci> [accessed 29 February 2016].
- Hubbell SP, Foster RB, O'Brien ST, Harms KE, Condit R, Wechsler B, Wright SJ, de Lao SL. 1999. Light-gap disturbances, recruitment limitation, and tree diversity in a neotropical forest. *Science* 283: 554–557.
- Huntingford C, Zelazowski P, Galbraith D, Mercado LM, Sitch S, Fisher R, Lomas M, Walker AP, Jones CD, Booth BBB *et al.* 2013. Simulated resilience of tropical rainforests to CO₂-induced climate change. *Nature Geoscience* 6: 268–273.
- IPCC. 2006. Chapter 4. Forest land. In: Eggleston S, Buendia L, Miwa K, Ngara T, Tanabe K, eds. *2006 IPCC guidelines for national greenhouse gas inventories, vol. 4, agriculture, forestry, and other land uses*. Hayama, Japan: Institute for Global Environmental Strategies.
- IPCC. 2013. Climate Change 2013: The Physical Science Basis. In: Stocker TF, Qin D, Plattner G-K, Tignor M, Allen SK, Boschung J, Nauels A, Xia Y, Bex V, Midgley PM, eds. *Contribution of Working Group I to the Fifth Assessment Report of the Intergovernmental Panel on Climate Change*. Cambridge, UK and New York, NY, USA: Cambridge University Press.
- Larjavaara M, Muller-Landau HC. 2010. Rethinking the value of high wood density. *Functional Ecology* 24: 701–705.
- Lawrence D, Vandecar K. 2015. Effects of tropical deforestation on climate and agriculture. *Nature Climate Change* 5: 27–36.
- Leigh EG, Windsor DM, Rand AS, Foster RB. 1990. The impact of the 'El Niño' drought of 1982–83 on a Panamanian semideciduous forest. In: Glynn PW, ed. *Global ecological consequences of the 1982–83 El Niño-Southern Oscillation*. Amsterdam, the Netherlands: Elsevier, 473–486.
- Lutz JA, Larson AJ, Swanson ME, Freund JA. 2012. Ecological importance of large-diameter trees in a temperate mixed-conifer forest. *PLoS ONE* 7: e36131.
- Manokaran N, LaFrankie JV, Kochummen K, Quah ES, Klahn J, Ashton PS, Hubbell SP, Chan HT. 1990. Methodology for the fifty hectare research plot at Pasoh Forest Reserve. *Research Pamphlet, Forest Research Institute of Malaysia* 104: 1–69.
- Markestijn L, Poorter L. 2009. Seedling root morphology and biomass allocation of 62 tropical tree species in relation to drought- and shade-tolerance. *Journal of Ecology* 97: 311–325.
- McDowell NG, Allen CD. 2015. Darcy's law predicts widespread forest mortality under climate warming. *Nature Climate Change* 5: 669–672.
- McDowell NG, Bond BJ, Hill L, Ryan MG, Whitehead D. 2011. Relationships between tree height and carbon isotope discrimination. In: Meinzer FC, Lachenbruch B, Dawson TE, eds. *Size and age related changes in tree structure and function*. Dordrecht, the Netherlands: Springer, 255–286.
- Muller-Landau HC, Condit RS, Chave J, Thomas SC, Bohlman SA, Bunyavejchewin S, Davies S, Foster R, Gunatilleke S, Gunatilleke N *et al.* 2006a. Testing metabolic ecology theory for allometric scaling of tree size, growth and mortality in tropical forests. *Ecology Letters* 9: 575–588.
- Muller-Landau HC, Condit RS, Harms KE, Marks CO, Thomas SC, Bunyavejchewin S, Chuyong G, Co L, Davies S, Foster R *et al.* 2006b. Comparing tropical forest tree size distributions with the predictions of metabolic ecology and equilibrium models. *Ecology Letters* 9: 589–602.
- Nepstad DC, Tohver IM, Ray D, Moutinho P, Cardinot G. 2007. Mortality of large trees and lianas following experimental drought in an Amazon forest. *Ecology* 88: 2259–2269.
- Phillips OL, van der Heijden G, Lewis SL, López-González G, Aragão LEOC, Lloyd J, Malhi Y, Monteagudo A, Almeida S, Dávila EA *et al.* 2010. Drought–mortality relationships for tropical forests. *New Phytologist* 187: 631–646.
- Powell TL, Galbraith DR, Christoffersen BO, Harper A, Imbuzeiro HMA, Rowland L, Almeida S, Brando PM, da Costa ACL, Costa MH *et al.* 2013. Confronting model predictions of carbon fluxes with measurements of Amazon forests subjected to experimental drought. *New Phytologist* 200: 350–365.
- Roberts J, Cabral OMR, Aguiar LFD. 1990. Stomatal and boundary-layer conductances in an Amazonian terra firme rain forest. *Journal of Applied Ecology* 27: 336–353.
- Rowland L, da Costa ACL, Galbraith DR, Oliveira RS, Binks OJ, Oliveira AA, Pullen AM, Doughty CE, Metcalfe DB, Vasconcelos SS *et al.* 2015. Death from drought in tropical forests is triggered by hydraulics not carbon starvation. *Nature* 528: 119–122.
- Ryan MG, Phillips N, Bond BJ. 2006. The hydraulic limitation hypothesis revisited. *Plant, Cell & Environment* 29: 367–381.
- Schielti J, Martins D, Emilio T, Souza PF, Levis C, Baccaro FB, da Veiga Pinto JLP, Moulatlet GM, Stark SC, Sarmiento K *et al.* 2016. Forest structure along a 600 km transect of natural disturbances and seasonality gradients in central-southern Amazonia. *Journal of Ecology* 104: 1335–1346.
- Sitch S, Huntingford C, Gedney N, Levy PE, Lomas M, Piao SL, Betts R, Ciais P, Cox P, Friedlingstein P *et al.* 2008. Evaluation of the terrestrial carbon cycle, future plant geography and climate-carbon cycle feedbacks using five Dynamic Global Vegetation Models (DGVMs). *Global Change Biology* 14: 2015–2039.
- Snyder PK, Delire C, Foley JA. 2004. Evaluating the influence of different vegetation biomes on the global climate. *Climate Dynamics* 23: 279–302.
- Swenson NG, Enquist BJ. 2007. Ecological and evolutionary determinants of a key plant functional trait: wood density and its community-wide variation across latitude and elevation. *American Journal of Botany* 94: 451–459.
- US DOE. 2012. *Research priorities for tropical ecosystems under climate change workshop report*, DOE/SC-0153. US Department of Energy Office of Science.
- West GB, Enquist BJ, Brown JH. 2009. A general quantitative theory of forest structure and dynamics. *Proceedings of the National Academy of Science, USA* 106: 7040–7045.
- Wolfe BT, Sperry JS, Kursar TA. 2016. Does leaf shedding protect stems from cavitation during seasonal droughts? A test of the hydraulic fuse hypothesis. *New Phytologist* 212: 1007–1018.
- Wright SJ. 1991. Seasonal drought and the phenology of understory shrubs in a tropical moist forest. *Ecology* 72: 1643–1657.
- Wright SJ, Kitajima K, Kraft NJB, Reich PB, Wright IJ, Bunker DE, Condit R, Dalling JW, Davies SJ, Díaz S *et al.* 2010. Functional traits and the growth–mortality trade-off in tropical trees. *Ecology* 91: 3664–3674.
- Zhang Y-J, Meinzer FC, Hao G-Y, Scholz FG, Bucci SJ, Takahashi FSC, Villalobos-Vega R, Giraldo JP, Cao K-F, Hoffmann WA *et al.* 2009. Size-dependent mortality in a Neotropical savanna tree: the role of height-related adjustments in hydraulic architecture and carbon allocation. *Plant, Cell & Environment* 32: 1456–1466.

Supporting Information

Additional Supporting Information may be found online in the Supporting Information tab for this article:

Fig. S1 Size scaling of stem density, aboveground live biomass C, aboveground woody productivity and woody mortality using biomass allometries from Chave *et al.* (2005).

Fig. S2 Size scaling of mean individual $C_{ag, live}$, individual diameter growth, individual biomass C growth and stem mortality rate.

Fig. S3 Size scaling of stem density, aboveground live biomass C, aboveground woody productivity and woody mortality on a non-linear scale.

Table S1 List of species classified as deciduous in this study along with source of deciduous observation

Table S2 Ecosystem-level C variables for all three sites during non-El Niño census periods using biomass allometries from Chave *et al.* (2005)

Table S3 Adjusted woody mortality values for the 1981–1985 Barro Colorado Island census period

Table S4 Demographic rates and C cycle variables by size class for each site and census period

Table S5 Fitted parameters corresponding to Fig. 1

Table S6 Fitted parameters corresponding to Fig. 2

Methods S1 Methods for classifying deciduous species.

Methods S2 Corrections to forest census data and exclusion of outliers.

Methods S3 Demographic variables.

Please note: Wiley Blackwell are not responsible for the content or functionality of any Supporting Information supplied by the authors. Any queries (other than missing material) should be directed to the *New Phytologist* Central Office.



About New Phytologist

- *New Phytologist* is an electronic (online-only) journal owned by the New Phytologist Trust, a **not-for-profit organization** dedicated to the promotion of plant science, facilitating projects from symposia to free access for our Tansley reviews and Tansley insights.
- Regular papers, Letters, Research reviews, Rapid reports and both Modelling/Theory and Methods papers are encouraged. We are committed to rapid processing, from online submission through to publication 'as ready' via *Early View* – our average time to decision is <26 days. There are **no page or colour charges** and a PDF version will be provided for each article.
- The journal is available online at Wiley Online Library. Visit **www.newphytologist.com** to search the articles and register for table of contents email alerts.
- If you have any questions, do get in touch with Central Office (np-centraloffice@lancaster.ac.uk) or, if it is more convenient, our USA Office (np-usaoffice@lancaster.ac.uk)
- For submission instructions, subscription and all the latest information visit **www.newphytologist.com**